Quantitative Studies on the Polarization Optical Properties of Living Cells II. The Role of Microtubules in Birefringence of the Spindle of the Sea Urchin Egg

Y. HIRAMOTO, YUKIHISA HAMAGUCHI, YÔKO SHÔJI, THOMAS E. SCHROEDER, SHUMEI SHIMODA, and SOICHI NAKAMURA

Biological Laboratory, Tokyo Institute of Technology, Tokyo 152, Japan; and Friday Harbor Laboratories, University of Washington, Friday Harbor, Washington 98250. Dr. Nakamura's present address is Department of Cell Biology, National Institute for Basic Biology, Myodaijicho, Okazaki 444, Japan.

ABSTRACT Birefringence of the mitotic apparatus (MA) and its change during mitosis in sea urchin eggs were quantitatively determined using the birefringence detection apparatus reported in the preceding paper (Hiramoto et al., 1981, *J. Cell Biol.* 89:115–120). The birefringence and the form of the MA are represented by five parameters: peak retardation (δ_p), trough retardation (δ_t), interpolar distance (D_1), the distance (D_2) between chromosome groups moving toward poles, and the distance (D_3) between two retardation peaks. Distributions of birefringence retardation and the coefficient of birefringence in the spindle were quantitatively determined in MAs isolated during metaphase and anaphase. The distribution of microtubules (MTs) contained in the spindle was determined in isolated MAs assuming that the observed birefringence of the spindle is attributable to the form birefringence caused by regularly arranged MTs. The distribution coincided fairly well with the distribution of MTs in isolated MAs determined by electron microscopy. Under the same assumption, the distribution of MTs in the spindle in living cells during mitosis was determined. The results show that the distribution of MTs and the total amount of polymerized tubulin (MTs) in the spindle change during mitosis, suggesting the assembly and disassembly of MTs as well as the dislocation of MTs during mitosis.

Since the pioneering work of Runnström (26) and Schmidt (31, 32), the mitotic figures of many kinds of living cells have been known to be birefringent. Improvement of polarization microscope technique has made it possible to measure the variation of birefringence retardation within the mitotic apparatus (MA) and its change during mitosis (34, 35). Inoué (13) found that the mitotic spindle consists of many birefringent fibers by polarization microscopy. Development of electron microscopy has revealed that a number of microtubules (MTs) are oriented in the pole-to-pole direction in the spindle and in radial direction in the aster, so that it has been generally assumed that the spindle fibers and astral rays observed by light microscopy consist of MTs. Sato et al. (30) demonstrated that the birefringence of the spindle isolated from the sea-star oocyte was mainly attributable to the MTs; they demonstrated the quantitative coincidence of observed and theoretical birefringence retardation of the spindle immersed in media of various refractive indices, based on the theories of Wiener (38) and Bragg and Pippard (1) on the birefringence of mixed bodies. However, it is undecided whether the spindle birefringence in living cells is solely attributable to MTs (e.g., see references 4 and 25).

If the birefringence of the spindle is mainly attributable to MTs, it may be possible to follow the behavior of MTs in the spindle in living cells from birefringence measurements. MTs are considered to play important roles in mitotic events such as chromosome movement and spindle elongation, but they are invisible by ordinary light microscopy. We undertook the

THE JOURNAL OF CELL BIOLOGY · VOLUME 89 APRIL 1981 121-130

present study to obtain quantitative data on the birefringence of mitotic apparatus and its change during mitosis in the sea urchin egg. We conclude that the birefringence of the isolated spindle results mainly from the form birefringence of aligned MTs. We have estimated changes in distribution of the number of MTs in the spindle during mitosis from our quantitative birefringence measurement of the spindle in living cells.

MATERIALS AND METHODS

Materials

Observations and measurements were made of fertilized eggs and isolated mitotic apparatuses of the sand dollar *Clypeaster japonicus*. Eggs were deprived of fertilization membranes and hyaline layers by treating with 1 M urea solution for 1–2 min shortly after insemination, washed four times with Ca-free artificial seawater, and then kept in Ca-free artificial seawater.

Mitotic apparatuses (MAs) were isolated by the glycerol/Mg^{2+}/Triton X-100 method (29) or the glycerol/tubulin method (28) at room temperature.

Observation and Measurement of Birefringence Retardation

A semiautomated birefringence detection apparatus was reported in detail in the previous paper (11). A drop of egg suspension was put on a strain-free slide. Glass rods of 60 to 80-μm diameter supported a cover slip that compressed the eggs to 50–65% of their original (~120 μm) diameters. In this condition, mitosis and cleavage proceeded normally and the axis of the mitotic spindle was formed parallel to the planes of the slide and the cover slip. The eggs were in contact with the slide and the cover slip over flat area of ~100-μm diameter, which sufficiently revealed the MA in the cell. For isolated MAs, the cover slip was supported on a strain-free slide by pieces of cover slip (~150-μm thickness). The slide was set on the stage of the apparatus with the azimuth of the spindle axis of the MAs to be measured at 45° with respect to the vibration direction of the polarizer. The lenses included a × 40 rectified objective (NA = 0.65; Nippon Kogaku K. K., Tokyo, Japan) and a rectified condenser (f = 8 mm, NA = 1.15 or f = 16 mm, NA = 0.52, Nippon Kogaku K. K.). Observation and photography were made by illuminating the entire microscope field with red light (>600-nm wavelength), while the retardation measurement was made for a small square area (2 × 2 μm^2) at the center of a 5-μm-square area illuminated by green light (546-nm wavelength). These two wavelengths of light were mixed on a dichroic mirror set under the polarizer and partially separated on another dichroic mirror set above the ocular to permit observation of the entire microscope field with simultaneous measurement of the birefringence retardation.

The birefringence retardation was determined from the intensity of light emerging from the 2-μm-square area mentioned above, when the compensator (Brace-Köhler compensator; Nippon Kogaku K. K.) was set at a definite angle, by reference to the relation between the light intensity and compensator angle which had been determined beforehand for a reference area without birefringence (11). In measuring the birefringence of the MA in living cells, an area in the egg cytoplasm near the MA was used as the reference area, where both the intensity of stray light and the attenuation of the light intensity are practically the same as those of the area of MA. In measurements of the isolated MA, a nonbirefringent area at the periphery of the MA was used as the reference because the attenuation of light is almost the same as by the MA.

The variation of retardation with distance along the spindle axis or along lines perpendicular to the axis (cross lines) was determined by measuring the light intensity when the slide was moved in the direction of the spindle axis or the direction perpendicular to the axis at a constant speed (8 μm/s). The stage-driving mechanism was described in the previous paper (11).

In isolated MAs, the retardation of various sites in the same MA was also determined from the angle of the compensator giving minimum light intensity (extinction angle, r_0) by equation $\delta_2 = -\delta_1 \sin 2r_0$, where δ_2 is the retardation for the sample area and δ_1 is the retardation of the compensator (24.7 nm or 27.7 nm for light of 546-nm wavelength).

Determination of the Coefficient of Birefringence

The coefficient of birefringence of the spindle at various distances from the spindle axis was determined by the method described by Hiramoto et al. (12) for determining the refractive index of the egg protoplasm. In this calculation, it was assumed that the spindle is composed of many concentric cylindrical shells with uniform birefringence of a definite thickness (0.8 μm) from the center after smoothing the retardation curve. Using a programmable calculator (HP-67; Hewlett-Packard Co., Palo Alto, Calif.), the coefficient of birefringence of the outermost shell was first determined, then the coefficient of the next shell was determined using the coefficient of the first shell, and so on until the coefficients of all shells were determined.

Estimation of the Number of MTs in the Spindle from Retardation Data

The relative amount of birefringent material in the spindle was estimated from data of birefringence retardation, assuming that (*a*) the density of the birefringent material is proportional to the coefficient of birefringence and (*b*) the optical axis of the material is parallel to the spindle axis at any region of the spindle. Because the retardation represents the integral of the coefficient of birefringence of the distance along the ray, the relative amount of birefringent material found in a cross section of the spindle was represented by the integral (M) of the retardation with respect to the distance along the line crossing the spindle axis at right angles, such that

$$M = \int_{-\infty}^{\infty} \Gamma(x)\, dx, \tag{1}$$

where $\Gamma(x)$ is the retardation at distance x on that line from the spindle axis. The distribution pattern of birefringent material along the axis of the spindle can be represented by M values at various cross sections of the spindle, without defining the nature of the material in detail. If the M value is integrated with respect to the distance along the spindle axis from pole to pole, we obtain the relative amount of birefringent material in the spindle corresponding to "volume-birefringence" introduced by Marek (18).

If it is further assumed that the spindle birefringence is entirely attributable to the MTs aligned in parallel to the spindle axis, the number of MTs in the spindle is estimated by applying the theories of Wiener (38) and Bragg and Pippard (1) to the birefringence of the spindle as follows (cf. reference 30). According to Bragg and Pippard (1) and Sato et al. (30), the coefficient of birefringence (B) of a mixed body made up of a number of oriented rodlets in a uniform medium is given by

$$B = I + [n_2^2 + f(n_1^2 - n_2^2)]^{1/2} - \left[n_2^2 + \frac{f(n_1^2 - n_2^2)}{1 + (1-f)\{(n_1^2 - n_2^2)/n_2^2\}/2}\right]^{1/2}, \tag{2}$$

where I is the coefficient of intrinsic birefringence, n_1 is the refractive index of the rodlets, n_2 is that of the medium, and f is the volume fraction occupied by the rodlets. When f is sufficiently small as compared with unity ($f \ll 1$),

$$B = I + \frac{(n_1^2 - n_2^2)^2}{2n_2(n_1^2 + n_2^2)} f. \tag{3}$$

Because the coefficient of intrinsic birefringence (I) is considered to be proportional to volume fraction (f) of rodlets, the coefficient of the total birefringence (B) is proportional to f. If it is assumed that the birefringence of the spindle is attributable to MTs regularly arranged in the spindle where Eq. 2 is applicable,

$$B = I + \frac{(n_1^2 - n_2^2)^2}{2n_2(n_1^2 + n_2^2)} A\bar{n}, \tag{4}$$

in which I is the coefficient of intrinsic birefringence of the MTs; n_1 and n_2 are refractive indices of the MT and the medium, respectively; A is the area of cross section of the MT; and $\bar{n}$ is the number of MTs per unit area of the cross section. Substituting 3.0×10^{-12} cm^2 calculated from the dimensions of the cross section of MT (24 nm in outer diameter and 14 nm in inner diameter; cf. reference 3) for A, 1.512 for n_1 (according to reference 30) and 1.345 (refractive index of the isolation medium) for n_2 into Eq. 3, the coefficient of birefringence of isolated spindle (B_I) is given by

$$B_I = I + (6.2 \times 10^{-14})\bar{n}_I, \tag{5}$$

where $\bar{n}_I$ is the number of MTs per unit area of the cross section of the isolated MA. (Subscript I means isolated MA and subscript L means MA in living cell in the present paper.)

In the case of the spindle in the living cell, the refractive index of the protoplasm surrounding MTs should be used as n_2. It is calculated, from the refractive index of the spindle (1.365 in *Clypeaster* egg [12]) and the volume occupied by the MTs in the spindle (0.5–1%, see below), to be 1.364, because the refractive index of the mixed body is given by the second or the third term of the

right side of Eq. 2. Substituting this value for n_2 into Eq. 3, the coefficient of birefringence of the spindle in the living cell (B_L) is given by

$$B_L = I + (4.8 \times 10^{-14})\bar{n}_L. \quad (6)$$

If it is further assumed that the coefficient of intrinsic birefringence (I) is negligible as compared with the total coefficient of birefringence (B_I and B_L), the number of MTs per unit cross section of the spindle is given by

$$\bar{n}_I = (1.61 \times 10^{13})B_I \quad (7)$$

and

$$\bar{n}_L = (2.08 \times 10^{13})B_L. \quad (8)$$

If the areal integral of the coefficient of birefringence over the cross section of the spindle (viz. the integral of the retardation along the cross line) is M_I in the isolated spindle and M_L in the spindle in the living cell, the total numbers of MTs in the cross section (N_I and N_L) are given by

$$N_I = (1.61 \times 10^{13})M_I \quad (9)$$

and

$$N_L = (2.08 \times 10^{13})M_L. \quad (10)$$

Errors introduced by assumptions used for derivation of above equations will be examined in the Discussion.

Observation of Differential Interference Microscopy

To confirm cytological events in living eggs, we observed them with a differential interference microscope (Biophot with differential interference optics, Nippon Kogaku K. K.; and in early experiments, BHB-333-N, Olympus Optical Co., Tokyo, Japan). Photomicrographs were taken of the same egg at intervals, using Kodak Panatomic X film. For some eggs, the slide was repeatedly transferred from the stage of the birefringence detection apparatus to the stage of the differential interference microscope for extended comparisons of cytology and birefringence. To do this, we adjusted the mechanical stage of each microscope before the start of an experiment so that the egg to be measured appeared at the center of the optical field in each case. In isolated MAs, chromosomes could be clearly observed through the viewfinder of the birefringence detection apparatus.

Electron Microscopy

Isolated MAs were fixed by adding 0.2 ml of 10% redistilled glutaraldehyde (final concentration = 2%) to 1 ml of isolation medium. After 15 min, this fixative was replaced by 1% osmium tetroxide/0.4 M sodium acetate, pH 7.0, for 30 min. After three changes of 70% ethanol, the MAs were stained by incubating in 1% uranyl acetate in 70% ethanol for 2 h. Dehydration was completed with ethanol and propylene oxide and a small volume of isolated MAs in propylene oxide was layered onto 1 ml of Epon in a polypropylene microcentrifuge tube. MAs were forced out of the propylene oxide and into the Epon by centrifuging at 5,000 g for 10 min. Propylene oxide was then removed.

Epon containing the MAs was scooped out of the centrifuge tube onto a flat sheet of polypropylene and allowed to spread in a desiccator for 12 h. The spread film of Epon was then polymerized at 60°C while still in a desiccator.

Individual MAs could be analyzed very carefully for mitotic stage and orientation with a Nomarski differential interference microscope (Carl Zeiss, Oberkochen, W. Germany; see Fig. 6). Selected MAs were cut out of the sheet, mounted with the MA axis upright, reinforced with additional Epon where necessary, and sectioned transversely. Serial sections of 0.25 μm were obtained with a diamond knife; every section in a complete series was collected and/or recorded. Sections were examined in a Philips EM 300 electron microscope operated at 100 kV with a 35-μm aperture. They were not stained after sectioning.

Sections displaying unobscured cross sections of MAs were examined; some of these representing important levels were photographed at × 13,000. Large photomontages printed at × 34,000 were arranged so that all MTs in a given cross section could be counted. The positions of these sections were determined by referring to the section numbers, the distances from sections containing the centrosomes and other distinctive markers, particularly chromosomes, that could be related to the light micrograph of the MA.

RESULTS

Birefringence of the MA during Mitosis

Fig. 1 correlates birefringence retardation measurements along the spindle axis with the cytological appearance of the same MA in a compressed living egg. Birefringence retardation along the axis exhibits a pattern of change that corresponds to the stage of mitosis. As previously described by Swann (34, 35), the birefringence is positive in the direction of the spindle axis

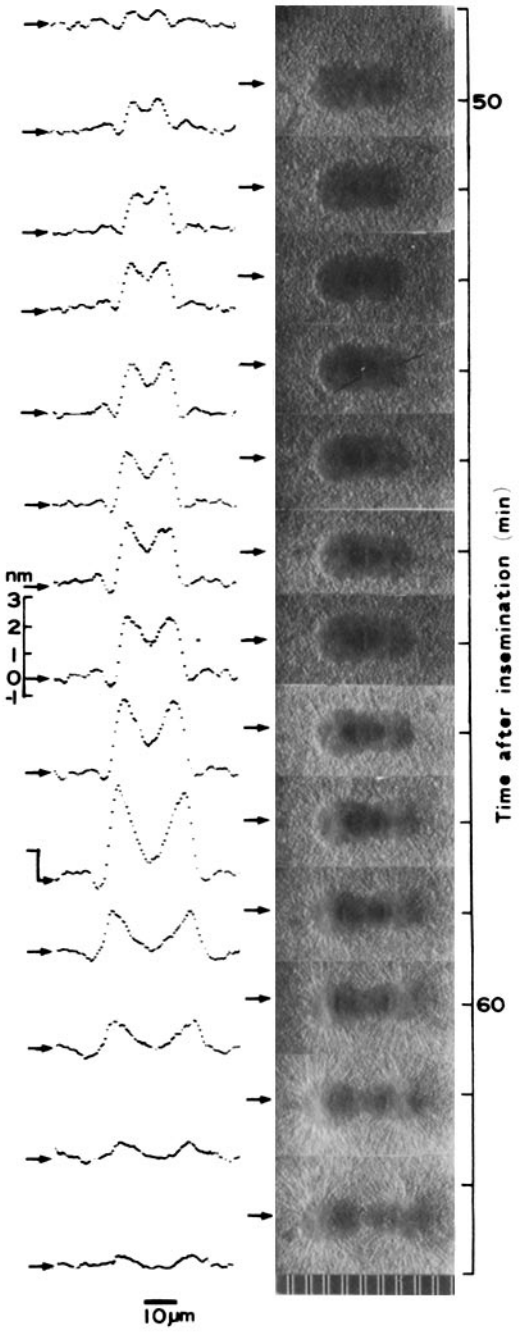

FIGURE 1 A series of oscillograph records of the distribution along the spindle axis of birefringence retardation of the MA in a living egg and differential interference micrographs of the same egg during mitosis. The oscillograph records and the micrographs were taken at the time indicated by arrows (cf. vertical scale on the right of the figure showing the time after insemination). The retardation scale for the eighth record is common for all the records.

and displays a pair of peaks straddling the equatorial plane. Birefringence retardation decreases away from the peaks, reaching an intermediate level at the equator and nearly disappearing at the poles. The height of the peaks of retardation increases during prometaphase and reaches a maximum at mid-anaphase before decreasing again. The height of the trough in the equatorial plane reaches a maximum at the beginning of anaphase, and then decreases.

Fig. 2 shows changes in the peak retardation (δ_p) and trough retardation (δ_t) together with the distance between the centers of asters (interpolar distance, D_1), the distance between separating chromosome groups (D_2) and the distance between the two peaks (D_3) averaged for 8–12 examples. The distance (D_4) between the points showing minimum retardation at the poles in oscillograph records coincided with the interpolar distance (D_1) determined in differential interference micrographs of the same egg. In averaging these characteristics, curves of their changes with time in individual eggs were averaged so that the moments when D_2 reaches 15 μm were taken as the time origin, and means and standard deviations of these characteristics were computed every minute. The curves of peak retardation shown in Fig. 2 are similar to those reported by Inoué and Sato (15) and Stephens (33), whereas they do not coincide with the results of Swann (34, 35), who concluded that the retardation reaches the maximum at metaphase. It can be seen in Fig. 2 that δ_p and δ_t increase in parallel during prometaphase and metaphase. It can also be seen in Fig. 2 that $(D_1 - D_3)/2$, the distance between the point of peak retardation and the pole, is almost unchanged during prometaphase, metaphase, and early anaphase, and that the distance between the chromosome group and the pole, $(D_1 - D_2)/2$, is unchanged during early telophase and gradually increases during late telophase.

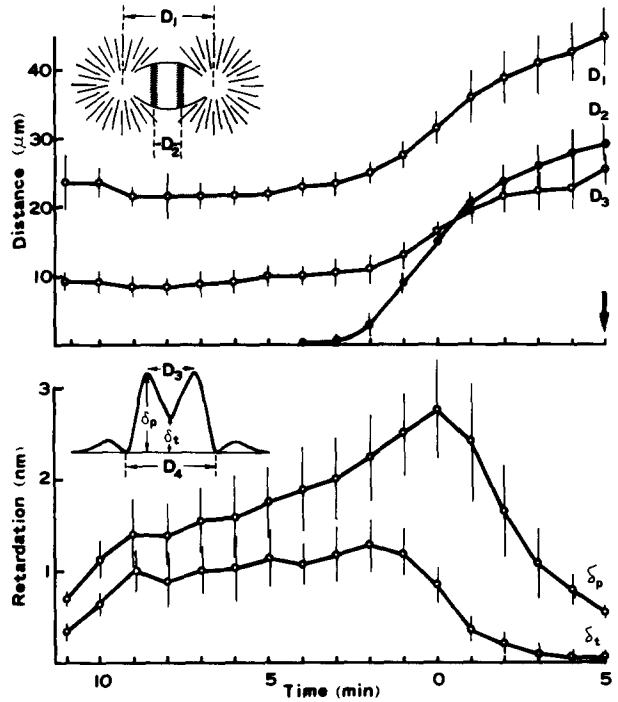

FIGURE 2 Averaged changes in the peak retardation (δ_p) and trough retardation (δ_t) together with the distances between the centers of asters (D_1), between the separating chromosome groups (D_2), and between the two retardation peaks (D_3) of the MAs in living cells. Circles with vertical bars indicate means and standard deviations. *Insets* schematically show parameters δ_p, δ_t, D_1, D_2, and D_3. The change in the distance (D_4) between the points of minimum retardation (cf. *inset*) is not shown in the graph, because it practically coincides with the change in D_1. The origin of time scale is defined as the time when the distance between separating chromosome groups is 15 μm, which practically corresponds to the time when the ratio of δ_t to δ_p is 0.3 (see the text).

The birefringence of astral rays is positive with respect to their axis, as already reported by previous investigators (e.g., see references 32 and 34). Small retardation peaks at the sides of the records in Fig. 1 at 53–57 min result from the birefringence of astral rays radiating in the direction of the spindle axis. The area showing birefringence expands as mitosis proceeds, corresponding to the growth of asters.

Birefringence of Isolated MAs

Fig. 3 shows a typical result of the birefringence retardation of an anaphase MA isolated by the glycerol/Mg^{2+}/Triton X-100 method (29). The pattern of retardation along the spindle axis in the MA (cf. Fig. 3*b*) was similar to that of the MA in a living egg at the same stage. Detailed analysis of 9 isolated anaphase MAs and 11 isolated metaphase MAs revealed that both the interpolar distance and the distance between retardation peaks in isolated MAs were almost the same as those of MAs in living eggs at the same stage. Both the peak retardation and the retardation at the equatorial plane in isolated MAs were larger than those in MAs in a living cell at the same stage. However, the peak retardation in isolated MAs nearly coincides with that in living MAs when the latter is multiplied by 1.3, which is the ratio of 6.2×10^{-14} in Eq. 5 to 4.8×10^{-14} in Eq. 6 for correcting the difference in refractive index of the medium surrounding the MA. The retardation at the equatorial plane in isolated MAs was slightly smaller than 1.3 times the retardation at the equatorial plane in living MAs.

The retardation was also determined at various points on the spindle axis in isolated MAs from the compensator angle giving minimum light intensity (extinction angle). Retardation values thus obtained practically coincided with values obtained from the light intensity when the compensator angle remains constant. This implies that determining the retardation by the latter method introduces a negligible error because of the

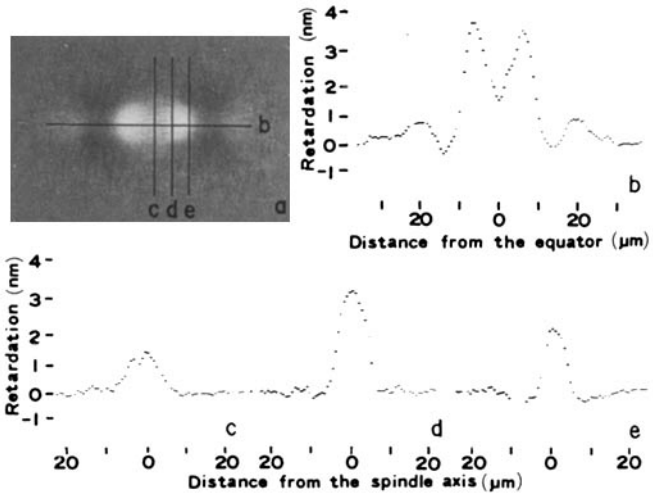

FIGURE 3 Birefringence retardation of an anaphase MS isolated by the glycerol/Mg^{2+}/Triton X-100 method. Retardation in *b* is measured along the spindle axis indicated by *b* in the polarization micrograph shown in *a*. Retardations in *c*, *d*, and *e* were measured along the cross lines indicated by *c*, *d*, and *e* respectively, in the micrograph *a*.

difference in absorption and scattering of light between the sample area and the reference area.

The peak retardation and the variation in retardation in MAs isolated by the glycerol/tubulin method (28) were similar to those in MAs isolated by the glycerol/Mg^{2+}/Triton X-100 method (29).

Fig. 3 *c*, *d*, and *e* shows distributions of birefringence retardation along cross lines indicated by *c*, *d*, and *e*, respectively, in Fig. 3 *a*. The retardation displays a peak at the spindle axis and diminishes toward the periphery of the spindle. Retardation on various cross lines along the spindle axis is qualitatively similar, although the peak values are different, as is expected from the distribution curve along the spindle axis.

Coefficient of Birefringence of the MA

Fig. 4 shows the birefringence retardation and the calculated coefficient of birefringence for a cross line 4 μm from the equatorial plane of the spindle in an isolated anaphase MA. Separate calculations were made for each half of the section. The coefficient of birefringence is generally uniform near the center of the spindle, and it gradually falls toward the periphery. Similar curves of the coefficient of birefringence were obtained in other sections of the spindle (e.g., the equatorial plane).

The coefficient of birefringence at the center of the spindle was 1–2 × 10^{-4} in MAs isolated during metaphase or early anaphase. This value corresponds to 1.6–3.2 × 10^{9} MTs/cm^2 (16–32 MTs/μm^2) of the cross section of the spindle (cf. Eq. 6) and to 0.5–1 × 10^{-2} (0.5–1%) of the area coupled by MTs in the cross section (f value in Eqs. 1 and 2).

Distribution of Birefringent Material in Isolated Spindle and Estimation of MT Number from Birefringence Data

Fig. 5 shows the integrated values of retardation (M) at various sections of an isolated anaphase spindle, representing the distribution of birefringence material in the spindle (cf. Eq. 1). Like the distribution pattern of retardation, the curve of an M value exhibits a pair of peaks straddling the equatorial plane. The distance between the two peaks in anaphase MAs was larger than that in metaphase MAs.

Because the relation between an M value and the number of MTs is given by Eq. 9, the distribution shown in Fig. 5 represents directly the distribution of the number of MTs (cf. right-hand vertical scale in Fig. 5), if it is further assumed that the spindle birefringence can be attributed entirely to the form birefringence of oriented MTs.

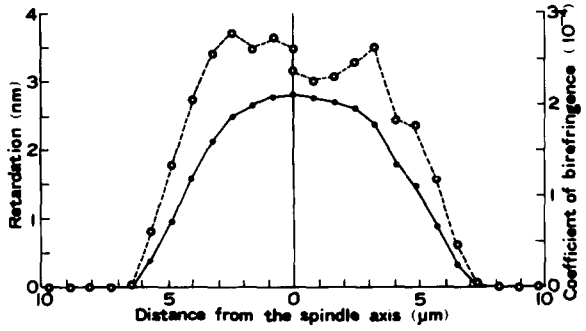

FIGURE 4 The distributions of birefringence retardation and the coefficient of birefringence in the section 4 μm away from the equatorial plane of the spindle in an isolated anaphase MA. The coefficients of birefringence (open circles) were calculated for each half of the distribution of retardation (closed circles) in the section, assuming axial symmetry of the spindle structure.

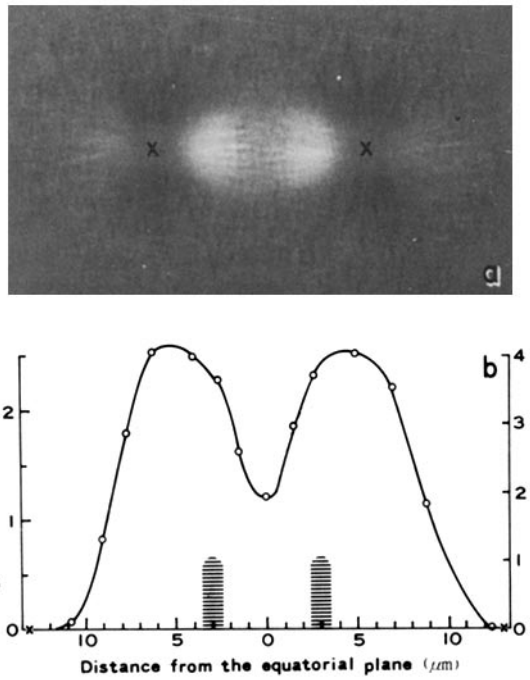

FIGURE 5 The distribution along the spindle axis of the number of MTs in an isolated anaphase MA determined from birefringence data. The amounts of birefringent material in cross sections are expressed by the integral of the retardation with the distance along the cross line (cf. left scale). The number of MTs in cross section (cf. right scale) is calculated assuming that the birefringence of the spindle is solely the result of the form birefringence by MTs arranged in parallel to the spindle axis. (*a*) Polarization micrograph of the MA used in determining the MT number. × 1,100. (*b*) Distribution of the MT number. The positions of chromosome groups are shown by hatched rectangles, and crosses indicate the centers of asters.

If the number of MTs in cross section is integrated along the entire length of the spindle, we obtain the total length of the MT when all the MTs in the spindle are connected in series. The total length of MT was calculated to be 6.2 cm in spindle shown in Fig. 3. This value corresponds to 17.6 pg of polymerized tubulin, because the mass of a 1-cm MT is 2.83 pg if it is assumed that each MT consists of a helix of tubulin with a pitch of 8 nm and 13 dimer molecules of 1.05 × 10^{5} daltons per pitch (cf. references 3 and 24). This is comparable to the amount of tubulin (10–20 pg) calculated from electron microscope data by Cohen and Rebhun (2) and that (26.4 pg) calculated from biochemical data by Sakai (27) in MAs isolated from sea urchin eggs.

If the spindle birefringence in living cells arises from the form birefringence resulting from oriented MTs, the coefficient of their birefringence will be ~0.77 (4.8 × 10^{-14}/6.2 × 10^{-14}) (see Eqs. 5 and 6) times the coefficient of the isolated MAs, owing to the difference of proportional factors, provided that MTs present in living cells are well preserved during the isolation procedure. The birefringence retardation of the spindle in living cells is also expected to be ~0.77 times that of the spindle in the isolation medium. As already mentioned above, the peak retardation of the spindle in an isolated MA was in fact ~1.3 (=1/0.77) times the peak retardation in the spindle in a living cell at the same stage.

Number of MTs in the Spindle of the Isolated MA Determined by Electron Microscopy

MTs were counted as cross-sectioned profiles in photomontages representing selected levels along a complete series of sections of an isolated MA. Results of a complete series for mid-anaphase are shown in Fig. 6. The corresponding differential interference micrograph of the same MA before it was sectioned is shown in Fig. 6 *a*. The location of chromosomes is plotted together with the MT counts, and spindle poles are marked by crosses (Fig. 6).The location of a "spindle pole" in differential interference and electron micrographs is taken as the center of the dense central mass of the centrosome.

Both the absolute value of the MT number and its variation with the distance along the spindle axis shown in this figure coincide fairly closely with those of the isolated anaphase spindle in Fig. 5, which is at practically the same stage as the spindle in Fig. 6. These facts suggest that the birefringence of the isolated spindle mainly arises from the form birefringence resulting from a regular arrangement of MTs. However, the possibilities of a contribution of intrinsic birefringence and the presence of other birefringent elements are not excluded, as will be discussed later.

The numbers and distribution of MTs were also determined for metaphase MAs by electron microscopy and from birefringence data. The results from the two techniques again coincided well. By direct counting, the peaks at metaphase were ~3,000 MTs in the isolated metaphase MA and those at anaphase were about 3,500 MTs, as shown in Fig. 6. This difference is matched by the birefringence for isolated MAs at similar stages and for MAs in living cells as mentioned in later section (cf. Fig. 9).

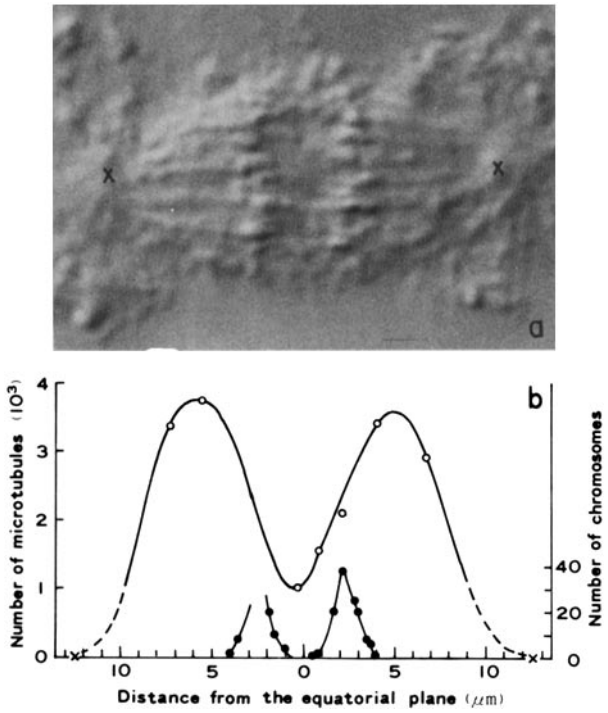

FIGURE 6 Distribution of the number of MTs in an isolated anaphase MA determined by electron microscopy. The number of MTs was counted in electron micrographs at various cross sections of the spindle. The number of chromosomes was also counted in sections. (*a*) Differential interference micrograph of the MA used in counting the MT number. × 2,000. (*b*) Distribution of the MT number. Open circles represent the number of MTs in the cross sections, closed circles represent the number of chromosomes, and crosses indicate the centers of asters.

The total number of chromosomes in *Clypeaster* eggs appears to be ~44, based in part on the number of dense chromosomes sometimes visible in isolated MAs viewed from a polar orientation by differential interference microscopy. The approximate number of kinetochore MTs in a half-spindle was determined to be 1,459, as follows: In one particularly favorable section of an anaphase MA (Fig. 6), 38 chromosomes could be discerned. Clusters of MTs appeared in positions previously occupied by chromosomes in several nearby sections and were inferred to be kinetochore-associated MTs. There were counted and were found to average 33.16 (n = 38; range, 14–57). Therefore, if there are 44 chromosomes, the total number of kinetochore MTs is 44 × 33.16 = 1,459.

Because the maximum number of MTs in a half-spindle of this MA was ~3,500, it appears that fewer than half are associated with kinetochores and the remainder are not in MTs present in this section.

Change in the Number of MTs in the Spindle during Mitosis

The number of MTs in a cross section of the spindle in living cells can be determined from the integral of retardation along the cross line using Eq. 10, if it is assumed that the spindle birefringence is attributable to the form birefringence of oriented MTs.

Retardation measurements were repeatedly made along the lines perpendicular to the spindle axis (cross lines) in the same egg during mitosis. In this experiment, successive measurements were made (*a*) along the spindle axis, (*b*) along the cross line passing the center of an aster (spindle pole), (*c*) along the cross line passing the point about one-sixth of the spindle length toward the equatorial plane from the pole, (*d*) along the cross line passing the point about one-third of the spindle length from the pole, and (*e*) along the cross line at the equatorial plane. Such a series of five successive measurements was repeated several times during mitosis.

Fig. 7 shows a typical result. In measurements along the cross line passing the spindle pole (second column), the retardation is low at the center and has a pair of troughs at points several micrometers from the center, indicating peaks of birefringence that are positive with respect to the axes of astral rays (here lying at right angles to the spindle axis). In measurements across the spindle (third, fourth, and fifth columns), a single peak was observed at the point crossing the axis. This resembles measurements across the spindle in isolated MAs (cf. Fig. 3 *c*, *d*, and *e*). Irregularities in records may be caused by discontinuities and partial overlap of spindle "fibers" and astral rays.

The retardation of the spindle in living cells must be measured rapidly, because birefringence changes during mitosis. Furthermore, retardation should be measured along many cross lines to obtain a distribution of MT number along the spindle axis similar to that of an isolated MA (e.g., Fig. 5). In this experiment, it takes ~6 s to obtain a single record representing the distribution along a cross line (scanning speed, 8 μm/s). Retardation changes very little within this short time, but it changes considerably between consecutive measurements. Consequently, the integrals of retardation along the cross line obtained from successive records are those for the spindle at different stages. In the present study, distributions of

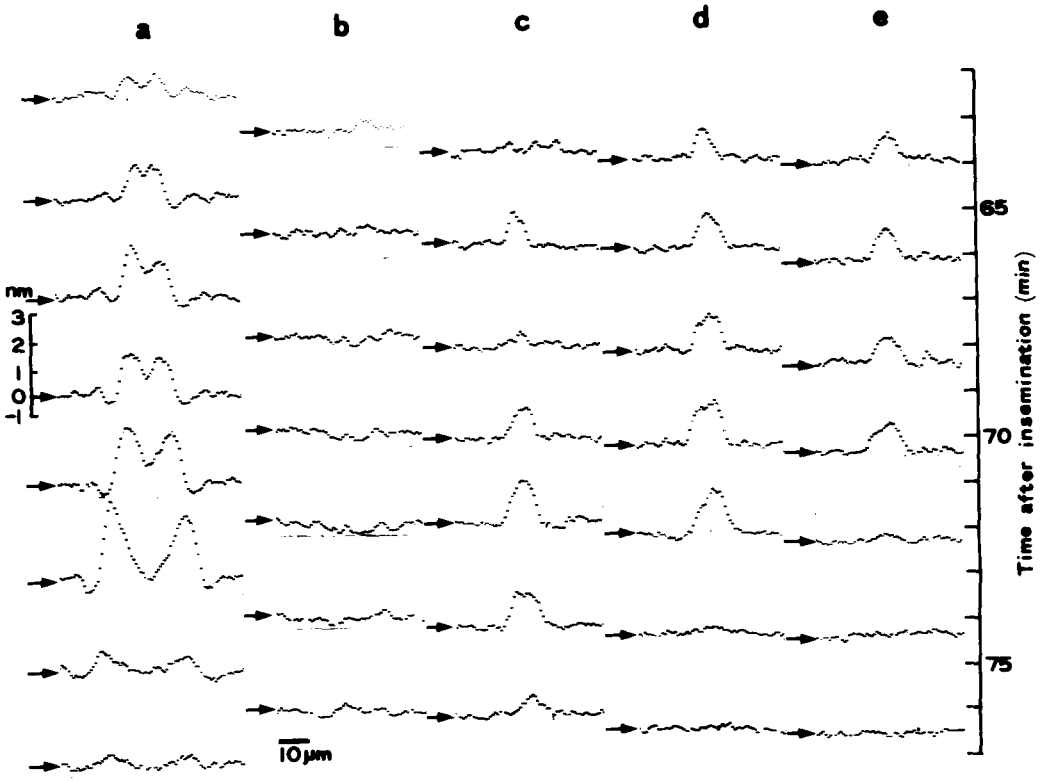

FIGURE 7 A series of oscillograph records of birefringence retardation along the spindle axis and the cross lines obtained from the same living egg during mitosis. The first column represents records of retardation along the spindle axis. Records of the second column are those of retardation along the cross line passing the center of one of the asters. Records of the third column are of retardation along the cross line passing the point on the spindle axis about one-sixth of the spindle length from the center of the aster. Records of the fourth column are retardation along the cross line passing the point on the spindle axis about one-third of the spindle length from the center of the aster. Records of the fifth column are of retardation along the cross line at the equatorial plane of the spindle.

MT number in the spindle at various stages of mitosis were estimated as follows.

Fig. 7 shows that the maximum retardation is different in each section of the spindle and that it changes with time, yet the width of the spindle is not particularly changed. In the following analysis, we define the "width" of the spindle as the value of the retardation integrated over the cross line divided by the maximum retardation in that section (in analogy with area divided by radius). If the maximum retardation and the width of the spindle are known at the same time in all the sections in the spindle, it should be possible to determine the distribution of integrals of retardation over the entire length of the spindle.

The width of the spindle was determined only at certain stages of mitosis and selected cross lines. Therefore we have estimated the changes in width along the length of the spindle as follows. Open circles in Fig. 8 *a* and *b* show the change in the width determined from the records of retardation at various sections in the spindle during mitosis. Using four successive records along cross lines (cf. Figs. 7 and 8), the widths at definite distance (2 μm, 4 μm, 6 μm, etc.) from the equatorial plane were estimated by interpolation (cf. closed circles in Fig. 8) and these values were plotted against time (closed circles in Fig. 8 *b*). After connecting all values at the same distance from the equatorial plane with smooth curves (dashed lines in Fig. 8 *b*), we arrived at estimated widths along the spindle at the stages that correspond to those when the variations in retardation with distance along the spindle axis were determined (vertical thin lines). Then values of width at these moments (dotted circles in Fig. 8 *b*) were plotted against the distance from the equatorial plane as shown in Fig. 8 *c*. Using the curves in Fig. 8 *c* indicating the "shape" of the spindle and variations in retardation with the distance along the spindle axis (cf. records in the first column in Fig. 7) that are regarded as the variations in the maximum retardation with the distance, we obtained values of the integral of retardation (B_L) at various cross lines of the spindle at various moments during mitosis. The number of MTs in cross section (N_L) was obtained by Eq. 10.

An example of these results is shown in Fig. 9. The positions of chromosome groups were estimated from the ratio of peak retardation to the retardation at the trough in the longitudinal scanning record (δ_p/δ_t) referring to the relation between δ_p/δ_t and D_2 shown in Fig. 2. The peak number of MTs along the length of the spindle increases during early anaphase, whereas the number at the equatorial plane decreases in this stage.

The total amount of polymerized tubulin represented by the total length of MTs in a spindle was obtained by integrating each curve with respect to the distance along the spindle length. A representative result is shown in Fig. 10. The total amount increases during metaphase and early anaphase and decreases during late anaphase and telophase. Because the total length of MTs changes during mitosis as shown in this figure, the formation and destruction of MTs as well as their dislocation in the spindle must be taken into consideration for interpreting the change in distribution of MTs.

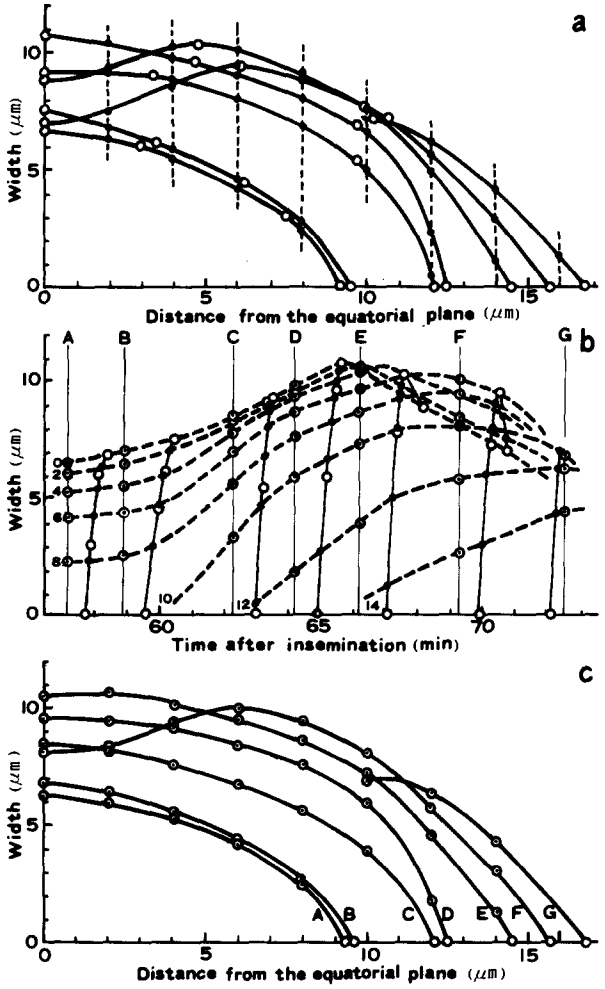

FIGURE 8 The change in the "width" of the spindle at various stages of mitosis in a living cell. Width is defined as the value of the integral of retardation with respect to the cross line divided by the maximum retardation in that cross line. Open circles in *a* and *b* show the width determined from the records of retardation at various sections in the spindle during mitosis (cf. Fig. 7). Closed circles in *a* show the width at definite distances from the equatorial plane, which is estimated by interpolation using four successive values (open circles in *a*) and are plotted on the graph showing the relation between the width and the time (closed circles in *b*). After connecting the values for the same distance from the equatorial plane with smooth curves (dashed lines in *b*), width values at the moments (vertical thin lines *A*, *B*, *C*, *D*, *E*, *F*, and *G*) when the distributions of retardation along the spindle axis were measured, are obtained at definite distances (dot circles). Then, width values at these moments are plotted against the distance in *c*, where the "shapes" of the spindle at various stages of mitosis are shown. *A* and *B*, prometaphase; *C* and *D*, metaphase; *E* and *F*, anaphase; *G*, telophase.

DISCUSSION

It has been shown in the present study that the distribution of MTs in the spindle can be determined from the data of birefringence in living spindles as well as isolated spindles of sea urchin eggs measured with the apparatus described in the foregoing paper (11). In the determination, we have assumed that (*a*) all MTs are aligned in parallel to the spindle axis, (*b*) the spindle birefringence can be attributed entirely to the form birefringence of MTs, and (*c*) this form birefringence can be calculated by the equation of Bragg and Pippard (1) (Eq. 2 of this paper) for a Wiener's mixed body consisting of parallel rodlets.

Although assumption *a* is not strictly valid, because MTs in the spindle are not exactly parallel to one another, the resulting error in birefringence is considered to be small. If MTs deviated 10° away from the spindle axis, the calculated retardation value would be only 5% from that predicted by the theory of birefringence (cf. reference 16). Some additional corrections may be required at terminal parts of the spindle where MTs converge upon the centrosome at an angle of >10° from the axis. Regarding assumption *b*, Rebhun and Sander (25) and Sato et al. (30) showed in MAs isolated from sea urchin, clam, and sea-star eggs that the birefringence of the spindle is mainly attributable to MTs, and they concur that most of the birefrin-

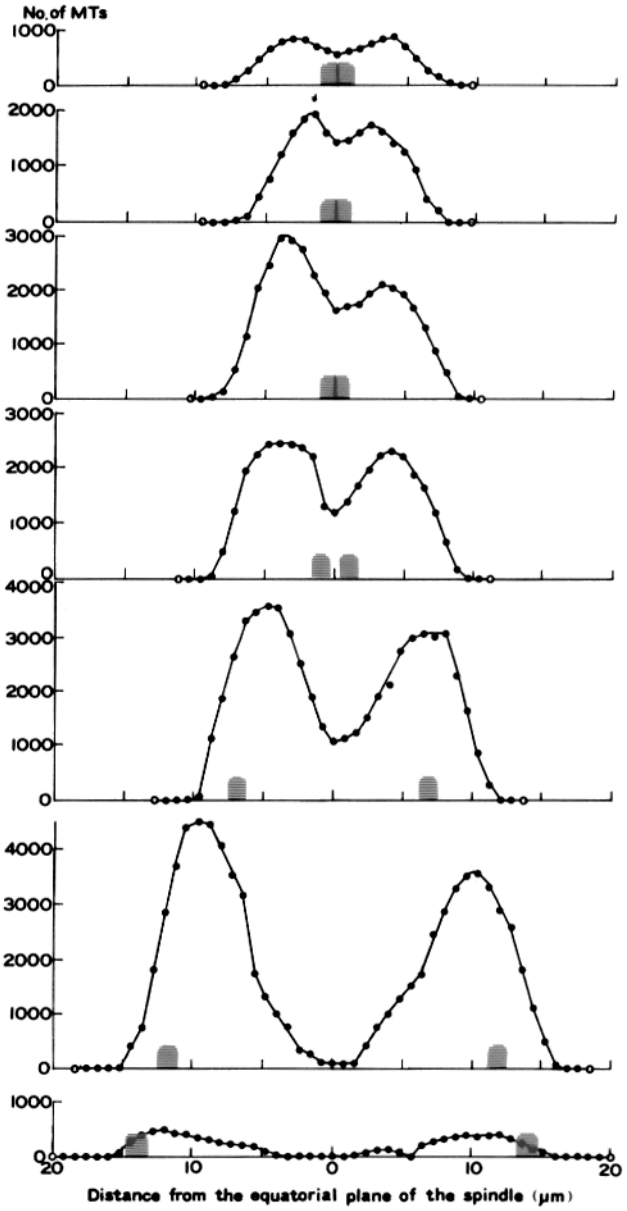

FIGURE 9 The distribution of the number of MTs in a living cell at various stages of mitosis. Numbers of MTs calculated from the products of the retardation and width of the spindle are plotted for various sections of the spindle. The positions of chromosome groups represented by hatched rectangles are estimated from the ratio of the trough retardation to the peak retardation by referring to the change in the mean ratio (δ_t/δ_p) during mitosis shown in Fig. 2.

gence is a result of the form birefringence. The applicability of the equation of Bragg and Pippard (1) (Eq. 2) was shown by Sato et al. (30). However, they assumed the cross sectional area of a MT to be ~200 nm^2, based on the dimensions of tubulin molecules forming MTs; in contrast, we have assumed it to be ~300 nm^2 by regarding the cross section as a ring 24 nm in outer diameter and 14 nm in inner diameter, based on electron microscope data (3). Although it has not been decided which assumption is more reasonable for the value to substitute into Eq. 2, one of the explanations is that the effective cross-sectional area of the MT in isolated spindles is smaller than that in living spindles, owing to partial loss or conformational change of its structure during the isolation procedure. According to Fig. 2 in Tilney et al. (36), MTs in isolated MAs measure 22 nm in outer diameter and 16 nm in inner diameter, which gives a cross-sectional area of ~180 nm^2.

Forer and co-workers (5–9) showed that the birefringence change does not parallel the change in microtubular structure in isolated MAs under hydrostatic pressure or cold treatment, suggesting the presence of birefringent nonmicrotubular components in MAs isolated by their methods. This result may not be crucial for assumption *b*, because it is possible that the partial loss or conformational change of the structure of the MA, which was not detectable by electron microscopy, occurred by the pressure or cold treatment, or that a new birefringent component was formed by deposition of nonmicrotubular cytoplasmic material in the spindle during their treatment. Such a possibility was shown by Sato et al. (30) in the spindle birefringence of sea urchin eggs fixed with a histological fixative.

It has been shown in the present study that the peak birefringence in isolated spindles coincides, within limits of individual variability, with that in living spindles at corresponding stages, if the differences in the refractive index of the surrounding medium between isolated MAs and living ones is corrected. This fact and the similarity in isolated and living MAs of the birefringence distribution along the spindle axis strongly suggest that MTs are well preserved during isolation procedures used in the present study (the glycerol/Mg^{2+}/Triton X-100 method [29] and the glycerol/tubulin method [28]) and that assumptions *a–c* above are reasonable.

Recently, the distribution of MTs in the spindle has been determined by counting MT numbers in electron micrographs of various spindle cross sections in different types of cells (10, 17, 19–23, 37). These investigations are important in understanding the structure of the spindle as a basis for the mechanism of mitosis. However, in this method, an elabolate procedure is required to obtain a series of data for even a single spindle, there are possible changes in the spindle structure resulting from untested sources of error during fixation for electron microscopy, and it is impossible to follow the dynamic changes in the spindle structure during mitosis for living cells. On the other hand, the method described in this paper for quantifying MT numbers in the spindle from birefringence measurements is applicable to a single living spindle. Although several assumptions are required for quantifying the MT number, the actual procedure is simpler and faster than electron microscopy. Use of a microcomputer would further simplify the data-processing steps in the present method. Because the present method and electron microscopy complement one another so well, however, the full exploration of dynamic changes in spindle structure during mitosis in various cells is expected to employ both methods.

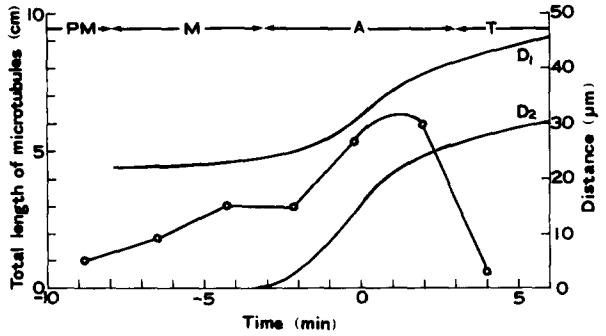

FIGURE 10 The change in the total amount of polymerized tubulin (MT) during mitosis in a living cell. The total amount (open circles) is represented by the length of the MT when all MTs in MA are connected in series. The distance (D_1) between the centers of asters and the distance (D_2) between the separating chromosome groups are also shown. The origin of time axis is defined in the same way as that in Fig. 2.

An exact correlation between the spindle birefringence and the mitotic stage has been achieved in this study by direct observation of chromosome behavior. This is possible because *Clypeaster* eggs are very transparent. The results shown in Fig. 2 indicate that the peak retardation reaches a maximum during mid-anaphase rather than metaphase (34, 35). It should be noticed in Fig. 2 that $(D_1 - D_3)/2$ (the distance of the peak retardation point from the pole of the spindle) is almost unchanged from the prometaphase through a definite stage during anaphase corresponding to the end of anaphase A (cf. reference 14), after which $(D_1 - D_2)/2$ (the distance of the chromosome group from the pole) is unchanged. Although the significance of these results is not altogether clear, they may be important in understanding the mechanisms of the spindle elongation and chromosome movement during mitosis.

Marek (18) introduced "volume-birefringence" (V-Br) as a new measure indicating the total amount of birefringent material in the spindle, which is proportional to the total amount of MTs. Although he calculated the V-Br to be $(\pi/12) \times$ length $\times$ width $\times$ retardation of the spindle (assuming that the spindle has an elliptical cross section of the equator and straight sides from equator to the poles), the V-Br should be calculated, to be exact, by integrating the coefficient of birefringence (BR) over the entire volume of spindle as described in the present paper, because the coefficient of BR is not uniform in the spindle. Marek (18) calculated the amount of MTs in the spindle to be 8.6 pg for *Melanoplus differentialis* and 26 pg for *Arphia xanthoptera*, assuming that the spindle BR is solely attributable to the form BR of aligned MTs. These values are comparable to the amount expressed by the total length (1 cm of which corresponds to 2.83 pg as mentioned above), of MTs (17.6 pg) in an isolated spindle obtained in the present study and in a living spindle shown in Fig. 10.

It has been shown in the present study that the total amount of BR corresponding to the total amount of polymerized tubulin (MTs) increases during prometaphase, metaphase, and early anaphase, reaches a maximum during anaphase, and decreases during late anaphase and telophase (cf. Figs. 9 and 10). The increase in the total amount of polymerized tubulin (MTs) has also been shown by limited electron microscope comparisons of isolated metaphase and anaphase MAs. The changes in the total amount of polymerized tubulin and in the distribution of MTs in the spindle during mitosis indicate that the structural changes during mitosis are explained neither by

the simple dislocation of preexisting MTs such as sliding between interdigitating MTs nor by the simple contraction and/or elongation of MTs. Assembly and disassembly of MTs as well as the dislocation of MTs must be taken into consideration.

We wish to thank Professors H. Sakai and S. Inoué for their numerous stimulating discussions of the present work and preparation of the manuscript, Mrs. M. S. Hamaguchi for her assistance in preparation of the mitotic apparatus, and Misaki Marine Biological Station for supplying the materials.

This work was supported by Grant-in-Aid for Developmental Scientific Research no. 284028 and Grants-in-Aid for Scientific Research nos. 348016 and 154246 from the Japan Ministry of Education, Science and Culture awarded to Y. Hiramoto and by U. S. Public Health Service Research Grant GM 19464 to T. E. Schroeder.

Received for publication 7 July 1980, and in revised form 18 November 1980.

REFERENCES

1. Bragg, W. L., and A. B. Pippard. 1953. The form birefringence of macromolecules. *Acta Crystallogr. Sect. B Struct. Cystallogr. Cryst. Chem.* 6:865–867.
2. Cohen, W. D., and L. I. Rebhun. 1970. An estimate of the amount of microtubule protein in the isolated mitotic apparatus. *J. Cell Sci.* 6:159–176.
3. Dustin, P. 1978. Microtubules. Springer-Verlag, Berlin.
4. Forer, A. 1978. Chromosome movements during cell-division: possible involvement of actin filaments. *In* Nuclear Division in Fungi. I. B. Health, editor. Academic Press, Inc., New York. 21–88.
5. Forer, A., and R. D. Goldman. 1969. Comparisons of isolated and *in vivo* mitotic apparatuses. *Nature (Lond.).* 222:689–691.
6. Forer, A., and R. D. Goldman. 1972. The concentrations of dry matter in mitotic apparatuses *in vivo* and after isolation from sea-urchin zygotes. *J. Cell Sci.* 10:387–418.
7. Forer, A., V. I. Kalnins, and A. M. Zimmerman. 1976. Spindle birefringence of isolated mitotic apparatus: further evidence for two birefringent spindle components. *J. Cell Sci.* 22:115–131.
8. Forer, A., and A. M. Zimmerman. 1976. Spindle birefringence of isolated mitotic apparatus analysed by pressure treatment. *J. Cell Sci.* 20:309–327.
9. Forer, A., and A. M. Zimmerman. 1976. Spindle birefringence of isolated mitotic apparatus analyzed by treatments with cold, pressure, and diluted isolation medium. *J. Cell Sci.* 20: 329–339.
10. Fuge, H. 1980. Microtubule disorientation in anaphase half-spindles during autosome segregation in crane fly spermatocytes. *Chromosoma (Berl.).* 76:309–328.
11. Hiramoto, Y., Y. Hamaguchi, Y. Shôji, and S. Shimoda. 1981. Quantitative studies on the polarization optical properties of living cells. I. Microphotometric birefringence detection system. *J. Cell Biol.* 89:115–120.
12. Hiramoto, Y., S. Shimoda, and Y. Shôji. 1979. Refractive index of the protoplasm in sea urchin eggs. *Dev. Growth Differ.* 21:141–153.
13. Inoué, S. 1953. Polarization optical studies of the mitotic spindles. I. The demonstration of spindle fibers in living cells. *Chromosoma (Berl.).* 5:487–500.
14. Inoué, S., and H. Ritter, Jr. 1975. Dynamics of mitotic spindle organization and function. *In* Molecules and Cell Movement. S. Inoué and R. E. Stephens, editors. Raven Press, New York. 3–30.
15. Inoué, S., and H. Sato. 1967. Cell motility by labile association of molecules. The nature of mitotic spindle fibers and their role in chromosome movement. *J. Gen. Physiol.* 50:259–292.
16. Jerrard, H. G. 1948. Optical compensators for measurement of elliptical polarization. *J. Opt. Soc. Am.* 38:35–59.
17. LaFountain, J. R., Jr., and L. A. Davidson. 1979. An analysis of spindle ultrastructure during prometaphase and metaphase of micronuclear division in *Tetrahymena. Chromosoma (Berl.).* 75:293–308.
18. Marek, L. F. 1978. Control of spindle form and function in grasshopper spermatocytes. *Chromosoma (Berl.).* 68:367–398.
19. McDonald, K. L., M. K. Edwards, and J. R. McIntosh. 1979. Cross-sectional structure of the central mitotic spindle of *Diatoma vulgare.* Evidence for specific interactions between antiparallel microtubules. *J. Cell Biol.* 83:443–461.
20. McDonald, K., J. D. Pickett-Heaps, J. R. McIntosh, and D. H. Tippit. 1977. On the mechanism of anaphase spindle elongation in *Diatoma vulgare. J. Cell Biol.* 74:377–388.
21. McIntosh, J. R., W. Z. Cande, and J. A. Snyder. 1975. Structure and physiology of the mammalian mitotic spindle. *In* Molecules and Cell Movement. S. Inoué and R. E. Stephens, editors. Raven Press, New York. 31–76.
22. McIntosh, J. R., W. Z. Cande, J. Snyder, and K. Vanderslice. 1975. Studies on the mechanism of mitosis. *Ann. N. Y. Acad. Sci.* 253:407–427.
23. McIntosh, J. R., K. L. McDonald, M. K. Edwards, and B. M. Ross. 1979. Three-dimensional structure of the central mitotic spindle of *Diatoma vulgare. J. Cell Biol.* 83: 428–442.
24. Olmsted, J. B., and G. G. Borisy. 1973. Microtubules. *Annu. Rev. Biochem.* 42:507–540.
25. Rebhun, L. I., and G. Sander. 1967. Ultrastructure and birefringence of the isolated mitotic apparatus of marine eggs. *J. Cell Biol.* 34:859–883.
26. Runnström, J. 1928. Die Veränderungen der Plasmabolloide bei der Entwicklungs-Erregung des Seeigeleies. *Protoplasma.* 4:338–514.
27. Sakai, H. 1978. The isolated mitotic apparatus and chromosome motion. *Int. Rev. Cytol.* 55:23–48.
28. Sakai, H., Y. Hiramoto, and R. Kuriyama. 1975. The glycerol-isolated mitotic apparatus: a response to porcine brain tubulin and induction of chromosome motion. *Dev. Growth Differ.* 17:265–274.
29. Sakai, H., S. Shimoda, and Y. Hiramoto. 1977. Mass isolation of mitotic apparatus in a glycerol/Mg^{2+}/Triton X-100 medium. *Exp. Cell Res.* 104:457–461.
30. Sato, H., G. W. Ellis, and S. Inoué. 1975. Microtubular origin of mitotic spindle birefringence. Demonstration of the applicability of Wiener's equation. *J. Cell Biol.* 67:501–517.
31. Schmidt, W. J. 1936. Doppelbrechung von Kernspindel und Chromosomen im lebenden, sichfurchenden Ei von *Psammechinus miliaris* (Müll.). *Ber. Oberhess. Ges. Natur- Heilk. Giessen Naturwiss. Abt.* 17:140–144.
32. Schmidt, W. J. 1937. Die Doppelbrechung von Karyoplasma, Meraplasma, und Zytoplasma. Borntraeger, Berlin.
33. Stephens, R. E. 1973. A thermodynamic analysis of mitotic spindle equilibrium at active metaphase. *J. Cell Biol.* 57:133–147.
34. Swann, M. M. 1951. Protoplasmic structure and mitosis. I. The birefringence of the metaphase spindle and asters of the living sea-urchin egg. *J. Exp. Biol.* 28:417–433.
35. Swann, M. M. 1951. Protoplasmic structure and mitosis. II. The nature and cause of birefringence changes in the sea urchin egg at anaphase. *J. Exp. Biol.* 28:434–444.
36. Tilney, L. G., J. Bryan, D. J. Bush, K. Fujiwara, M. S. Mooseker, D. B. Murphy, and D. H. Snyder. 1973. Microtubules: evidence for 13 protofilaments. *J. Cell Biol.* 59:267–275.
37. Tippit, D. H., D. Schultz, and J. D. Pickett-Heaps. 1978. Analysis of the distribution of spindle microtubules in the diatom *Fragilaria. J. Cell Biol.* 76:737–763.
38. Wiener, O. 1912. Die Theorie des Mischkörpers für das Feld der Stationären Strömung. *Abh. Math.-Phys. Kl. Saechs. Akad. Wiss.* 32:509–604.